ICEMS'2003

PROCEEDINGS OF THE SIXTH INTERNATIONAL CONFERENCE ON

ELECTRICAL MACHINES AND SYSTEMS

November 9-11, 2003, Beijing, China

Volume II

Edited by

Fangquan Rao Guobiao Gu

INTERNATIONAL ACADEMIC PUBLISHERS

WORLD PUBLISHING CORPORATION

X. Field Analysis and Computation

Iron Loss Analysis Method Considering Harmonics of Magnetic Flux Density Waveforms

Hyuk NAM[1], Jeong-Jong LEE[1], Ki-Chan CHANG[1], Jung-Pyo HONG[1], *Senior Member, IEEE*, and Jung-Ho LEE[2]

[1]Dept. of Electrical Eng., Changwon Nat'l Univ., #9 Sarim-dong, Changwon, Gyeongnam, 641-773, Korea
[2]Dept. of Electrical Eng., HANBAT Nat'l Univ., San16-1, DuckMyoung-dong, YuSeong-gu, Daejeon, 305-719, Korea
Phone: 82-55-2625966 Fax: 82-55-2639956 E-mail: haeggee@korea.com Website: http://ecad.eecu.net

***Abstract*-This paper deals with iron loss analysis method considering harmonics of magnetic flux density waveforms in the single-phase line-start permanent magnet synchronous motor. The iron loss is affected on the time rate of the change of magnetic flux density at the motor cores. The distribution and changes in magnetic flux densities of the motor are computed by using 2-D finite element method. Discrete Fourier Transform is used to analyze the magnetic flux density waveforms in each element of the analysis model. Iron losses in each element are evaluated using iron loss curves tested by Epstein test apparatus. The total iron loss can be obtained by the summation of the iron losses in all the elements.**

I. INTRODUCTION

Capacitor-run single-phase induction motor (SPIM) is widely used in household applications, because of the operation fed directly from the commercial single-phase voltage source without any control device. However, efficiency improvements are difficult, because the resistances and the induced currents in the conductor bars induce the slip power loss. On the other hand, single-phase line-start permanent magnet synchronous (LSPM) motors are essentially an induction motor with added permanent magnet material, i.e., these motors have a rotor cage for induction starting and permanent magnet, providing synchronous torque. Since the motor operates as a synchronous machine, the induced currents in the rotor are much smaller than that in an induction machine and, therefore, rotor power losses are significantly reduced. In addition, it is possible to achieve unity-power-factor performance, thereby reducing the stator currents and the corresponding losses [1]. In spite of the excellent performance of the LSPM motors, their optimal utilization requires attention to many aspects related to the machine design and performance. In this respect the calculation of iron losses, which can account for a significant component of the total loss, is particularly challenging since it requires an accurate prediction of the magnetic flux density distribution in both spatial and temporal coordinates, and the corresponding iron loss [2], [3]. In traditional ac machine theory the iron loss is viewed as being caused mainly by the fundamental frequency. Normally, under alternating flux conditions, the iron loss P_l in W/kg is separated into a hysteresis loss component P_h, and an eddy current component P_c, both in W/kg, as shown in equation (1).

$$P_l = P_h + P_c = k_h f B_m^{\alpha} + k_c f^2 B_m^2 \qquad (1)$$

where f and B_m are the frequency and the peak value of the magnetic flux density, respectively. k_e, k_h and α are constants provided by the manufacturer. This conventional method assumes sinusoidal variation of the magnetic flux density waveforms. Therefore, this method is not sufficiently accurate because the magnetic flux density waveforms are non-sinusoidal [3][4]. In order to take into account the harmonic effects of the magnetic flux density waveforms on the iron loss, accurate prediction of the magnetic flux densities throughout the stator and the rotor cores need to be performed [5].

This paper deals with the iron loss analysis method considering harmonics of the magnetic flux density waveforms using iron loss curves tested by Epstein test apparatus in the LSPM motor. The temporal and the spatial variations of the magnetic flux density waveforms are derived by performing 2-dimensional finite element method (2-D FEM). In this study, the skew effect is ignored. Discrete Fourier Transform (DFT) is used for the frequency analysis of the time-varying magnetic flux density waveforms at each element of the finite element (FE) analysis model. The iron losses at each element are calculated from iron loss data sheet that is expressed as iron loss curves according to frequencies and magnetic flux densities and tested by Epstein test apparatus. Finally, the total iron loss is obtained by the summation of the iron losses in all the elements. This result of the iron loss calculation is used for the accurate efficiency assumption of the LSPM in the steady state.

II. PROCEDURE FOR IRON LOSS ANALYSIS

The flow chart of the proposed method is shown in Fig. 1

A. Finite Element Analysis

The governing equation of improved finite element (FE) analysis from Maxwell's electromagnetic equation is as follows [5].

$$\nabla \times \nu\left(\nabla \times \vec{A}\right) = \vec{J}_0 - \sigma \frac{\partial \vec{A}}{\partial t} + \nabla \times \left(\nu \mu_0 \vec{M}\right) \qquad (2)$$

where ν is the magnetic reluctivity, $\vec{A}$ is the magnetic vector potential, $\vec{J}_0$ is the current density of the coil, σ is the rotor bar conductivity, μ_0 is the magnetic permeability of free space and $\vec{M}$ is the magnetization.

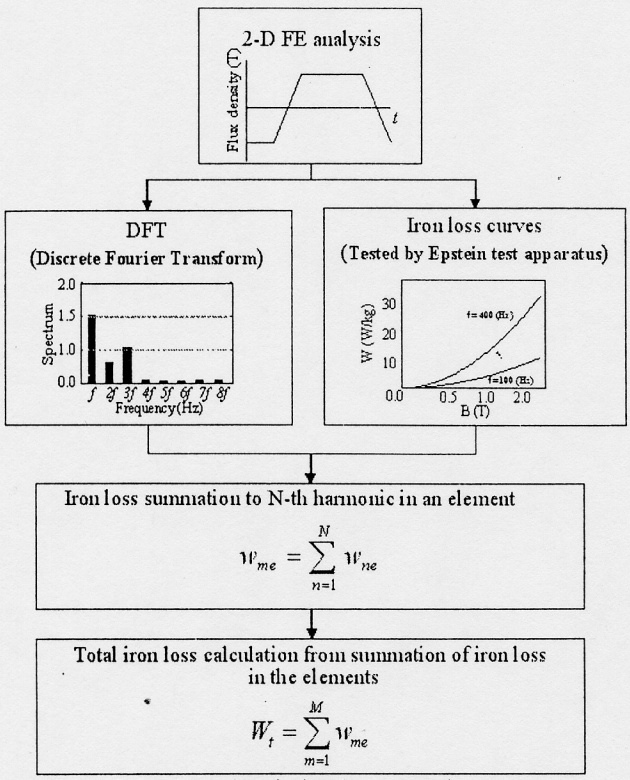

Fig. 1. Flow chart for iron loss calculation.

In equation (2), the winding current and the magnetic vector potential should be decided. Therefore, the voltage equation is demanded to decide these values.

Equation (3) and equation (4) show the voltage equations of the main and the auxiliary windings, respectively.

$$V = R_m I_m + L_m \frac{dI_m}{dt} + E_m \tag{3}$$

$$V = R_a I_a + L_a \frac{dI_a}{dt} + E_a + V_c \tag{4}$$

$$\frac{dV_c}{dt} = \frac{1}{C_r} I_c \tag{5}$$

where V is the input voltage, R_m, L_m, E_m, and I_m are the winding resistance, the end-coil leakage inductance, the electromotive force (EMF), and the winding current of the main winding, respectively. In addition, R_a, L_a, E_a, and I_a are those of the auxiliary winding, respectively. V_c in equation (5) is the voltage in the running capacitor.

B. DFT (Discrete Fourier Transform)

DFT can be expressed as equation (6).

$$B_{pk}(k) = \sum_{n=0}^{N-1} B_p(n) e^{j\frac{2\pi nk}{N}} \tag{6}$$

where k is the harmonic order, N is the number of the discrete data, $B_{pk}(k)$ is the peak value of the magnetic flux density of the k-th harmonic, and $B_p(n)$ is the magnitude of the point n *(n=0, 1, 2, …, N-1).*

III. Procedure For Iron Loss Analysis

A. Analysis Model and Experimental Results

Fig. 2 shows the cross-section of the analysis model. The motor has two windings, a main winding connected directly to the 115V, 60Hz supply, and an auxiliary winding connected to the supply via capacitor. Rotor has the permanent magnet, and the conductor bars inserted in the rotor as shown in Fig. 2.

Table I shows the experimental results at the rated condition. Total loss in the motor is about 21.00W including winding copper loss of 8.67W. Therefore, iron loss, stray load loss, and conductor loss in the rotor are about 12.33W, that is, the losses occupy about 58.7% in the total losses.

B. Analysis Results

Fig. 3 presents the iron loss curves of the magnetic material which is tested by Epstein test apparatus

As the rated currents are applied at the steady state, the distribution of the equipotential with angular position is shown in Fig. 4. Fig. 5, and Fig. 6 show the component magnetic flux density waveforms at different locations in the stator and the rotor, that is, e_1, e_2, and e_3 in Fig. 2, and the DFT results of the waveforms, respectively. In Fig. 6, e_1, and e_2 that represent positions in the stator yoke have equal frequency to the rotating magnetic field, and the tangential component of the magnetic flux density leads the normal component. On the other hand, the distribution of the magnetic fields of e_3 that shows a position in the rotor yoke are expressed as dc components because the rotation of the rotor synchronizes with that of the rotating magnetic field.

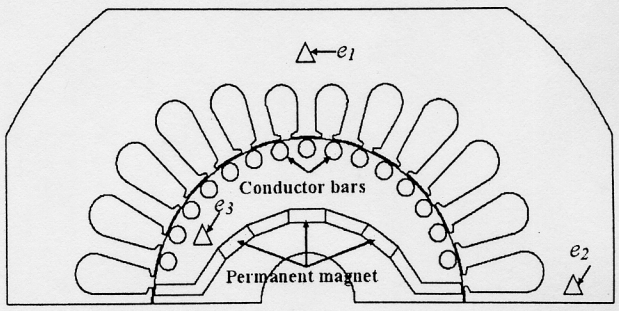

Fig. 2. LSPM Motor structure.

TABLE I
EXPERIMENTAL RESULTS AT THE RATED CONDITION

Input power (W)	Output power (W)	Winding copper loss (W)	Efficiency (%)
181.00	160.00	8.67	88.39

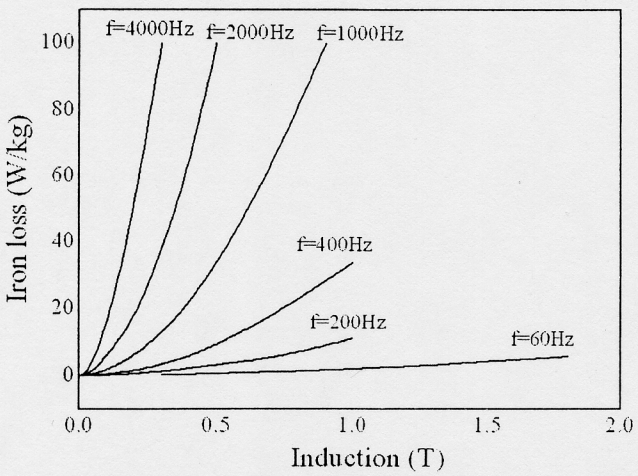

Fig. 3. Iron loss curves tested by Epstein test apparatus.

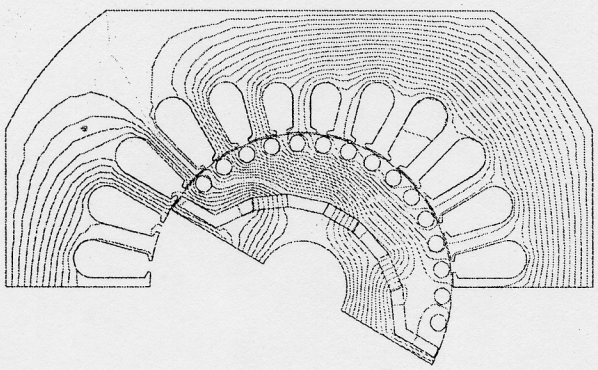

(a) Angular position 30 (deg.).

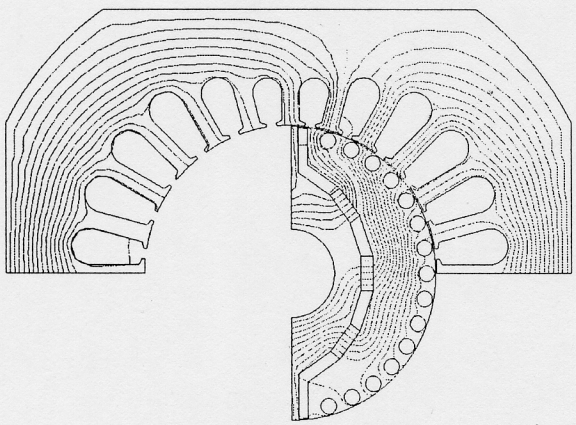

(b) Angular position 90 (deg.).

Fig. 4. Equipotential line at the steady state.

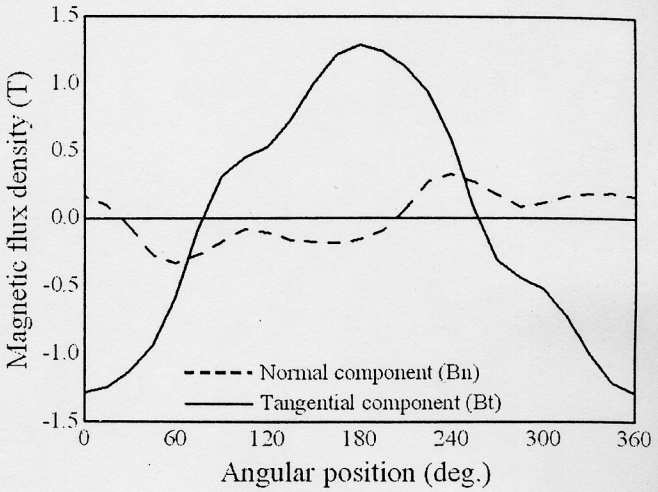

(a) e_1 in Fig. 2.

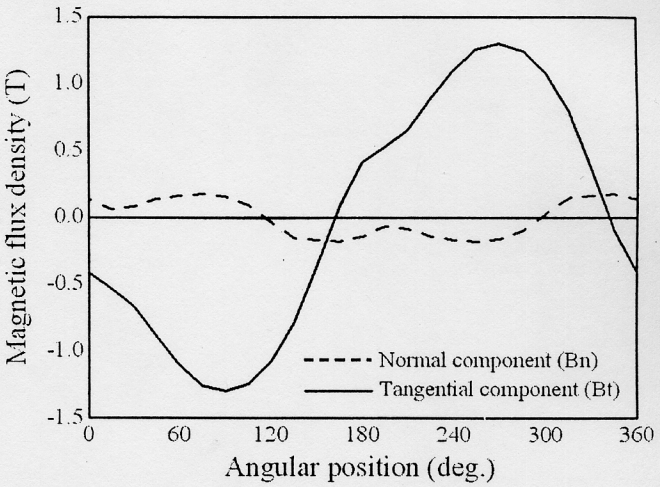

(b) e_2 in Fig. 2.

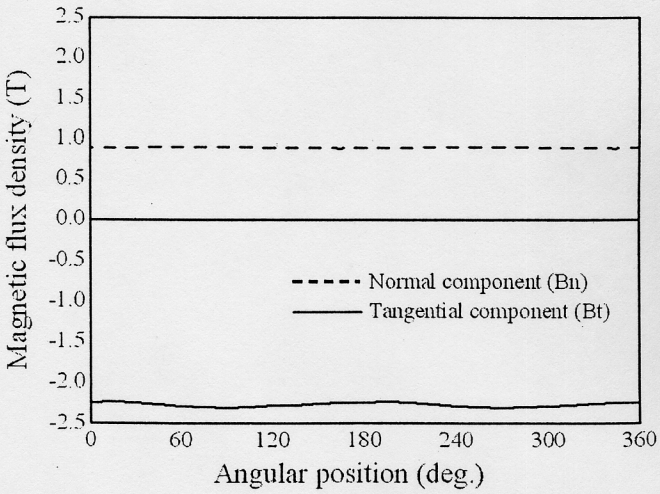

(c) e_3 in Fig. 2.

Fig. 5. Normal and tangential component waveforms of the magnetic flux density at selected sites.

Fig. 6, where the fundamental frequency is 60Hz, shows the harmonic components as well as the fundamental component frequency is contained in the magnetic flux density.

Fig. 7 presents the iron loss components from the fundamental component to the 12th harmonic component according to the harmonic order.

From the results, the total iron loss to the 12th harmonic component is 12.10W, and the losses except for the fundamental component is about 9.41W that occupies about 77.77% in the total iron loss. Therefore, it is very important to analyze the iron loss considering the harmonic components in the magnetic flux density waveforms. When the loss of 12.33W by the experiment is compared with the loss by the proposed method, the loss of 0.23W remains. It is supposed that the loss contains the iron loss by the harmonic components, not considered in the analysis, the stray load loss, and the conductor bar loss by the unbalanced magnetic field.

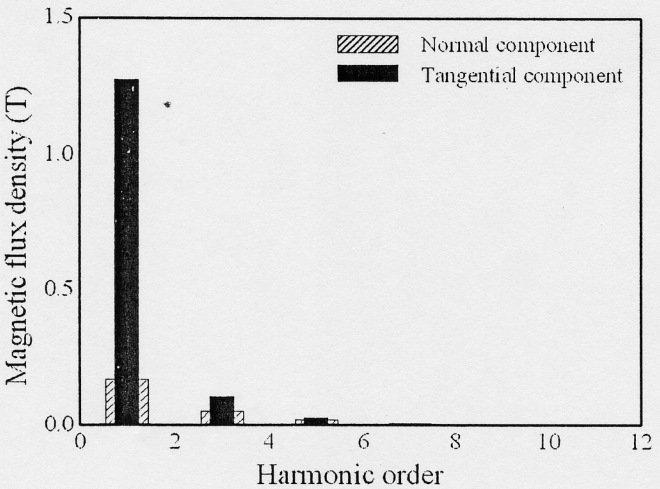

(a) e_1 in Fig. 2.

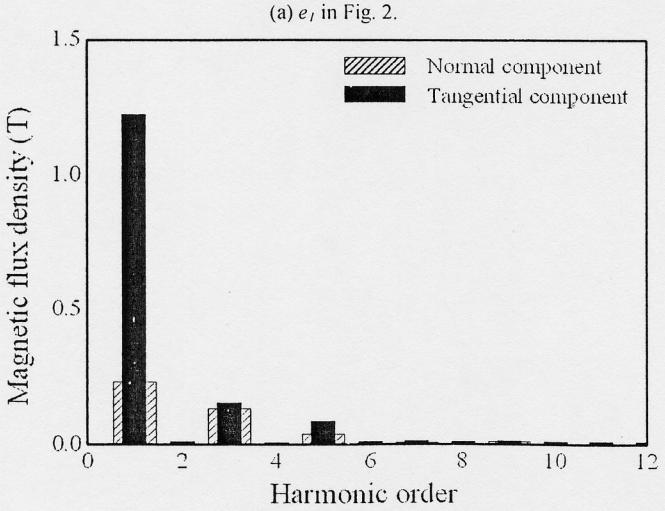

(b) e_2 in Fig. 2.

Fig. 6. Harmonic analysis results of the normal and tangential component waveforms at selected sites.

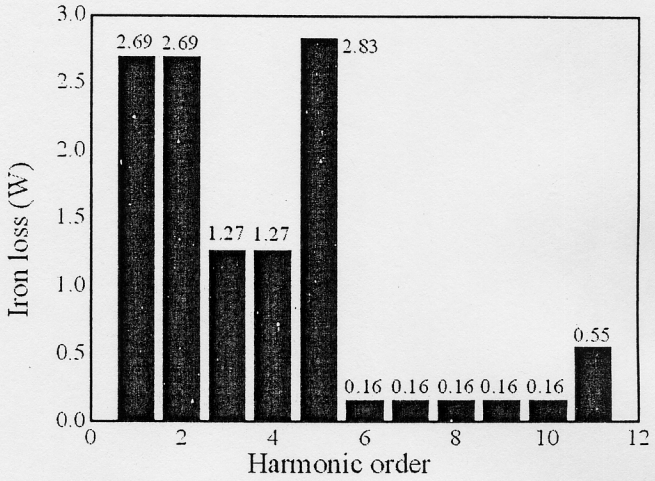

Fig. 7. Iron loss computation results with the harmonic order.

IV. CONCLUSIONS

This paper deals with the iron loss analysis method considering harmonics of the magnetic flux density waveforms.

DFT is used for the frequency analysis of the time-varying magnetic flux density waveforms calculated by 2-D FEM.

The iron losses of the harmonic components are calculated from iron loss curves tested by Epstein test apparatus.

From the analysis results, the total iron loss to the 12th harmonic component is 12.10W, and the loss except for the fundamental component is about 9.41W that occupy about 77.77% in the total iron loss. When the iron loss is compared with the loss of 12.33W, except for the winding copper loss of 8.67W by the experiment, the loss of 0.23W remains. It is supposed that the loss contains the iron loss by the harmonic components, not considered in the analysis, the stray load loss, and the conductor bar loss. Therefore, the accurate iron loss can be calculated as the harmonic order components are considered.

REFERENCES

[1] A. M. Knight, and C. I. McClay, "The design of high-efficiency line-start motors," *IEEE Trans. Ind. Applicat.*, vol. 36, no. 6, pp. 1555-1561, November/ December 2000.

[2] K. Atallah, Z. Q. Zhu, and D. Howe, "An improved method for predicting iron losses in brushless permanent magnet dc drives," *IEEE Trans. Magn.*, vol. 28, no. 5, pp. 2997-2999, September 1992.

[3] S. Inamura, H. Shibayama, and K. Sawa, "A simple estimation method of iron loss in switched reluctance motor, " in *Proc. COMPUMAG*, France, Evian, pp. IV-62-IV-64, July 2001.

[4] F. Deng, "An improved iron loss estimation for permanent magnet brushless machines, " *IEEE Trans. Energy Conversion*, vol. 14, no. 4, pp. 1391-1395, December, 1999.

[5] A. M. Knight, and J. C. Salmon, "Modeling the dynamic behaviour of single-phase line-start permanent magnet motors," *IEEE/IAS 34th Annual Meeting of Industry Applications Conference*, vol. 4, pp. 2582-2588, 1999.